NAIC-ID(RS)T-0510-95

NATIONAL AIR INTELLIGENCE CENTER

THERMAL SPOT TRACKING, FOLDING FFT
MODIFICATION FOR LASER PROPAGATION
IN TURBULENT ATMOSPHERE, AND
BEAM TRANSFORMATION OPTICS
(Selected Articles)

**Approved for public release:
distribution unlimited**

HUMAN TRANSLATION

NAIC-ID(RS)T-0510-95 12 Mar 96

MICROFICHE NR: 96C000223

THERMAL SPOT TRACKING, FOLDING FFT MODIFICATION FOR LASER PROPAGATION IN TURBULENT ATMOSPHERE, AND BEAM TRANSFORMATION OPTICS (Selected Articles)

English pages: 42

Source: Qiangjiguang Yu Zizishu (High Power Laser and Particle Beams), Vol. 4, Nr. 4, November 1992; pp. 513-515; 581-587; 612-620.

Country of origin: China
Translated by: Leo Kanner Associates
F33657-88-D-2188
Requester: NAIC/TATD/Bruce Armstrong
Approved for public release: distribution unlimited.

TABLE OF CONTENTS

GRAPHICS DISCLAIMER

All figures, graphics, tables, equations, etc. merged into this translation were extracted from the best quality copy available.

ATMOSPHERIC DISPERSION RELATED TO THERMAL SPOT TRACKING

Lu Qisheng, Liu Zejin, Jiang Zhiping,
Zhang Zhengwen, and Zhao Yijun

Department of Applied Physics
National University of Defense Technology
Changsha, Hunan 410073

ABSTRACT The propagating traces of two light beams of $\lambda_1 = 3.8\mu m$ and $\lambda_2 = 10.6\mu m$ were calculated in the atmosphere with spherical symmetrical index distribution of refraction, and the influence of the chromatic dispersion on the thermal spot tracking was discussed in this paper.

KEY WORDS atmospheric dispersion, light trace, light spot lock-in, thermal spot tracking.

I. Introduction

As light propagates in a medium, the refractivity distribution of the medium strongly affects the propagation path of light. Refractivity is related to the factors of the density, temperature and pressure of the medium. Moreover, refractivity is also related to factors of terrestrial gravitation, space environment, meteorology, terrain, and ecological environment. There have been numerous research achievements about these effects, compiled in related publications [1,2]. If only the terrestrial gravitation is considered, the distribution of refractivity with atmospheric height can be assumed as spherically symmetrical. Especially in some local environments,

this approximation is basically established.

At present, the problems of aiming and tracking with laser beams are often involved in scientific research and defense technology. In particular, the precise tracking of moving objects, and steadily locking with laser light spots onto a certain site of a moving object is very important. This precise tracking should adopt a closed cycle system to timely revise the tracking error in order to satisfy high-precision tracking requirements. When a moving object is illuminated with a laser beam, two kinds of radiation will be generated: one is diffused reflected light, and the other is the thermal radiation due to heating by the laser. Both kinds of radiation can be considered as the feedback signal of a closed-ring chain. The feedback signal using diffused reflected light is called echo tracking. The feedback signal using thermal radiation is called thermal-spot tracking. The basis for selecting the tracking scheme is how to upgrade the signal-to-noise ratio and to shorten the response time, among other elements. For example, the response is slow in the case of thermal-spot tracking as tens of ms are required to build up thermal spots. In the case of echo waves, the transmission time of light in air is the only consideration. In a shared-aperture tracking system, the diffused reflection of the system becomes the same frequency interference for echo tracking. However, in the case of thermal-spot tracking, the wavelength of thermal radiation can be used as the light wavelength of the feedback signal. Just by adopting the measure

of light filtering, a relatively high signal-to-noise ratio can be obtained.

In the scheme of thermal-spot tracking, the wavelength of the emitted light differs from the wavelength of the received signal light. With the effect of chromatic dispersion in the atmosphere, these two kinds of light propagate along the different paths; this will affect precise tracking. In the following, 3.8μm is used as the wavelength of the emitted light, and 10.6μm is used as the wavelength of the received light. Thus, an example is used to calculate the deviation of the transmission locus in the atmosphere. The effect of such deviation on thermal-spot tracking is discussed.

II. Propagation of Light Rays in Spherically Symmetric Atmosphere

Assume the refractivity distribution in the earth's atmosphere is related to height h above the ground, that is

$$n(r)=n(r_e+h) \tag{1}$$

In the equation, r_e is the earth's radius. When a laser beam is emitted upward from A on the ground with angle Φ_s (refer to Fig. 1), its path can be calculated with the light ray equation [3]:

$$\theta=D\int_{r_e}^{r}\frac{dr}{r\sqrt{n_\lambda^2(r)r^2-D^2}} \tag{2}$$

In the equation

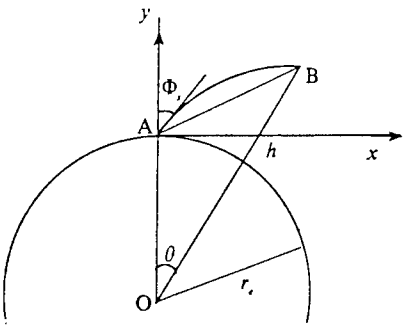

Fig. 1 The geometry of light line propagation in the atmosphere

$$D = n_\lambda(r_e) r_e \sin\Phi_s \tag{3}$$

$$n_\lambda(r) = 1 + N_\lambda(r) \tag{4}$$

$$N_\lambda(r) = \frac{p(r)}{t(r)}(0.7748 + 0.0046976\lambda^{-2}) \times 10^{-6} \tag{5}$$

Eq. (5) is adapted to the environment [1,2] $p(r_e) = 1.01325 \times 10^5 \text{Pa}$, $T(r_e) = 288.15\text{K}$. In the equation, the atmospheric pressure distribution p(r) with height has Pa as the unit; and the wavelength is given in μm. To calculate quantitatively, in Eq. (5) p(r)/t(r) is approximate with the ideal gas state equation, that is

$$\frac{p(r)}{t(r)} = k\rho(r) \tag{6}$$

In the equation, k is Boltzmann's constant.

By using the results of Appendix 2 in [4], an analytical function is (by trial fitting)

$$\rho = \rho(r_e) \times 10^{-h/17} \tag{7}$$

In the equation, h is the height from the ground, given in km. The condition is adaptable only within the range h=0 to 120km. Since

$$p(r_e)/T(r_e) = 351.64$$

therefore

$$\frac{p(r_e+h)}{T(r_e+h)} \approx 351.64 \times 10^{-h/17} \tag{8}$$

finally, we obtain

$$n_\lambda(r_e+h) = 1 + (272.45 + 1.652\lambda^{-2}) \times 10^{-(6+\frac{h}{17})} \tag{9}$$

Substitute Eqs. (3) and (9) in Eq. (9) to obtain the light path. It can be proved that the light path is a planar curve [3] in the plane included with angle Φ_s.

III. Calculation Results and Discussion

Assume λ_1=3.8μm and λ_2=10.6μm, and the initial emission angle Φ_s is 45°, r_e=6000km. From calculations, the laser (of two wavelengths) locus in air is shown in Fig. 2.

In the figure, the abscissa $X_{\lambda i} = (r_e+h)\sin\varphi_{\lambda i}$, and the ordinate $Y_{\lambda i} = (r_e+h)\cos\theta_{\lambda i} - r_e$. $X_{\lambda i}$ and $Y_{\lambda i}$ indicate the projections on the x- and y-axes. λ=3.8μm and 10.6μm. The laser emits a locus with Φ_s=45°. Fig. 2 exhibits $Y_{\lambda 1} - X_{\lambda 1}$ and $Y_{\lambda 2} - X_{\lambda 2}$. These are expressed in terms of deviations from the actual locus when emitted at 45°. This is to amplify the details of the deviation. Although in Fig. 2, m is used as the unit of the vertical axis, we are still unable to separate the light locus of the two

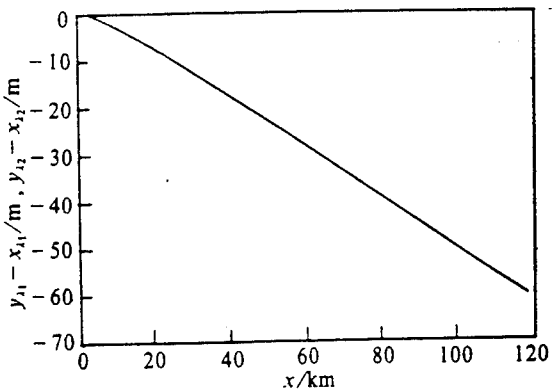

Fig. 2 The propagating trace of $\lambda_1 = 3.8\mu m$ and $\lambda_2 = 10.6\mu m$

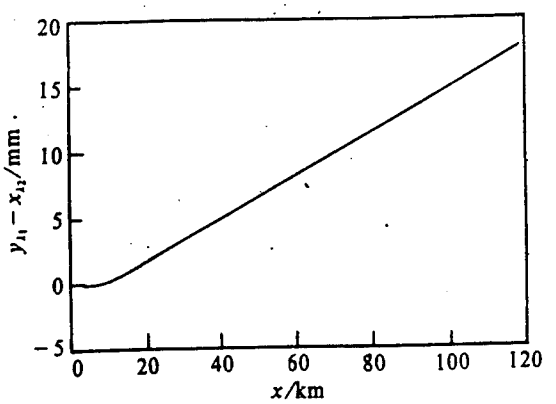

Fig. 3 The difference between of the propagating trace of the $\lambda_1 = 3.8\mu m$ and $\lambda_2 = 10.6\mu m$

wavelengths. Therefore, we plotted Fig. 3. In Fig. 3, the vertical coordinate has mm as the unit in terms of $Y_{\lambda 1} - Y_{\lambda 2}$. In addition, the numerical results corresponding to h=1, 3, 10, 100, and 120km, are listed in Table 1.

The propagation path of light is reversible in a medium. If from point A, a laser emits at the wavelength 3.8μm toward point B at the angle Φ_s to burn a thermal spot at point A, the 10.6μm radiation emitted by the thermal spot returns to point B with different light paths. As revealed from the calculation results mentioned above, the incident angle Φ_s toward point A in the path of 10.6μm irradiated light is smaller than Φ_s. If the system is so controlled that the laser (3.8μm) emits at the angle Φ'_s, then the laser light spot will move upward from point B. In such repeated cycles, the light spots cannot be locked, which will automatically leave the target. Angular revision should be made

Table 1 The data of light line trace with $\lambda_1 = 3.8\mu m$, $\lambda_2 = 10.6\mu m$, $\Phi_s = 45^\circ$

h/ km	X_{s1}/ km	$Y_{s1} - X_{s1}$/ m	X_{s2}/ km	$Y_{s2} - X_{s2}$/ m	$Y_{s1} - Y_{s2}$/ mm
1	0.99995	-3.532×10^{-2}	0.99995	-3.534×10^{-2}	-2.372×10^{-2}
3	2.99954	-2.913×10^{-1}	2.99954	-2.914×10^{-1}	-3.364×10^{-2}
10	9.99415	−2.461	9.99415	−2.461	5.338×10^{-1}
100	99.24261	−49.962	99.24259	−49.948	14.636
120	118.90544	−60.654	118.90542	−60.636	17.826

if precise locking is intended. If the target object moves at the velocity **v**, then the tracking system should rotate the light beam at the angular velocity $|\mathbf{v}/R|$ (with the direction $R \times \mathbf{v}$). Moreover, revisions are made from time to time on the path (or the emission angle). Only Eq. 2 is subjected to integration over time, and we can obtain $d\Theta/dt$, as well as the relationship between the velocity **v** and $d\Phi_s/dt$. When adopting the precise tracking scheme of thermal spot, we should establish the relationship between $d\Phi'_s/dt$ and $d\Phi_s/dt$. This is not the problem to be solved in this article, therefore this is omitted.

The first draft of the article was received on April 2, 1992; the final revised draft was received for publication on June 11, 1992.

REFERENCES

[1] 宋正方.应用大气光学基础，气象出版社，1990。

[2] 伏.耶.祖也夫.激光的大气传播，中国工程物理研究院，1990。

[3] M.玻恩，E.沃耳夫.光学原理，北京：科学出版社，1978, 167。

[4] K.q.康德拉捷夫等.高层大气热状态，北京：科学出版社，1964. 或 R. A. Minzner . Higher atmopsheric densities and temperatures demanded by Satellite and recent rocket measurements. Am. Rocket Soc., 1959.

FOLDING FFT MODIFICATION FOR LASER PROPAGATION IN THE TURBULENT ATMOSPHERE

Wang Yingjian and Wu Yi
Anhui Institute of Optics and Fine Mechanics,
P.O. Box 1125
Hefei 230031

ABSTRACT The traditional method of numerical simulations for laser beam propagation in the turbulent atmosphere is modified. A folding FFT treatment is put forward. High spatial frequency terms of the turbulent spectrum are sampled and low spatial frequency terms are revised using this treatment. Numerical simulation results show that the calculation speed and accuracy are both enhanced and the required computer memory is reduced. Also the numerical results reflect the real properties of strong and weak effects of the atmospheric turbulence.
KEY WORDS atmospheric turbulence, laser propagation, FFT method.

I. Introduction

Numerical calculations of the effects of turbulence in the atmosphere are one of the important aspects in studying the atmospheric transmission of lasers. These calculations relate to establishing a four-dimensional calculation program of the high-powered laser transmission in the atmosphere. The conventional simulation algorithm of the turbulent phase screen in the atmosphere is the limitation by the computer computational speed and internal memory. It is very difficult to ensure the

requirements of computational accuracy with regard to the turbulence spectrum as well as the total width of space sampling and sample density. Therefore, the information lost in the high- and low-frequency spectra of turbulence is very great. With regard to the optical effects of such loss, this involves the tilt of the light beam and scintillation of light intensity. It is even so with the intensive turbulence effects. Therefore some authors calculated turbulence effects by using various modified spectra [1,2]. The authors improved on the conventional simulation algorithm of the turbulence phase screen in the atmosphere and proposed a folding FFT algorithm, thereby solving the problem of numerically describing the turbulence spectrum in the calculation method. As revealed in the results of the numerical simulation of laser beam transmission in a turbulent atmosphere, this algorithm upgrades the computational speed and accuracy, lowers the requirements on computer internal memory, and more truly simulates the strong and weak effects of atmospheric turbulence. In the authors' view, this approach is helpful to constructing a four-dimensional computer program of high-powered laser transmission in the atmosphere, especially when considering the interaction of turbulent flow and thermal blooming.

II. Inversion of Turbulence Phase Screen

Generally, numerical simulation on the effects of atmospheric turbulence in laser transmission is carried out by

using the phase screen approximation [1-4]. In this approach, the turbulent atmosphere is divided into several layers along the direction in which the light beam is transmitted. The contribution of each layer amounts to changing the phase of the transmission light beam in that layer; however, the light beam is considered as transmitted in vacuo when the beam is between two layers. For the atmospheric turbulence layer with thickness Δz, the action on the phase perturbation difference of the light beam is:

$$\Delta\varphi = k\int_{z}^{z+\Delta z} \delta n(r, z')dz' \tag{1}$$

In the equation, $k=2\Pi/\lambda$ is the wave number; δn is the refractivity perturbation of the turbulent atmosphere; z is the transmission direction; r is the coordinate of the point as the light beam passes through the cross-sectional plane. The approximate conditions of the phase screen are as follows [1-4]: Δz is longer than turbulence correlation distance, but smaller than r_0^2/λ; r_0 is the transverse-direction coherence length of the turbulence. Due to the randomness of atmospheric turbulence, the phase screen is unable to be executed by using Eq. (1). The authors adopt the phase correlation function and density of the refractivity perturbation spectrum to invert the phase screen. The self-correlation definition of the phase screen is [5]:

$$B_{\varphi}(r_1, r_2) = <\Delta\varphi(r_1, z)\Delta\varphi(r_2, z)>$$

$$= k^2 \int\int_{z}^{z+\Delta z} <(\delta n(r_1, z_1)\delta n(r_2, z_2)> dz_1 dz_2 \qquad (2)$$

< > indicates the overall average of the system. Based on [1] and [5], there is:

$$<\delta n(r_1, z_1)\delta n(r_2, z_2)> = 2\pi C_n^2(z_1, z_2)\delta(z_1, z_2)\int\int_{-\infty}^{\infty} \Phi_n(\kappa_z = 0, \vec{\kappa})$$

$$\cdot \exp(i\vec{\kappa}\cdot\vec{\rho}) d^2\vec{\kappa} \qquad (3)$$

$C_n^2(z)$ is the vertical distribution of the structure constant of turbulence refractivity; $\delta(z)$ is the Dirac function; $\vec{\rho} = r_1 - r_2$, $|\vec{\kappa}| = (\kappa_x^2 + \kappa_y^2)^{1/2}$ is the conjugate variable of the Fourier transform domain of ρ; $\Phi_n(\kappa_z = 0, \vec{\kappa})$ is the density function of the refractivity fluctuation spectrum. With respect to the Kolmogorov spectrum [6]:

$$\Phi_n(\kappa) = 0.033\kappa^{-11/3}, \qquad \frac{2\pi}{L_0} \leqslant \kappa \leqslant \frac{5.92}{l_0} \qquad (4a)$$

l_0 and L_0 are, respectively, the internal and external dimensions of the turbulence. With respect to Von Karman spectrum [6]:

$$\Phi_n(\kappa) = 0.033(\kappa^2 + 4\pi^2/L_0^2)^{-11/6} \qquad (4b)$$

Substitute Eq. (3) into Eq. (2) and we obtain:

$$B_{\Phi}(\vec{\rho}) = 2\pi k^2 \int\int_{-\infty}^{\infty} \Phi_n(\kappa_z = 0, \vec{\kappa}) \exp(i\vec{\kappa}\cdot\vec{\rho}) d^2\vec{\kappa} \int_{z}^{z+\Delta z} C_n^2(z') dz' \qquad (5a)$$

Definition:

$$F_{\Phi}(\vec{\kappa}) = 2\pi k^2 \Phi_n(\kappa_z, \vec{\kappa}) \int_z^{z-\Delta z} C_n^2(z')\, dz' \qquad (5b)$$

We can see that $B_{\Phi}(\vec{\rho})$ and $F_{\Phi}(\vec{\kappa})$ are the conjugate Fourier transform functions. Thus, the light beam phase fluctuation screen induced by the turbulent atmospheric layer with a thickness (δz) can be generated by the conventional method [1,2]:

$$\Delta\varphi(r, z) = q \iint_{-\infty}^{\infty} g(\vec{\kappa}) F_{\Phi}^{1/2}(\vec{\kappa}) \exp(i\vec{\kappa} \cdot r)\, d^2\vec{\kappa} \qquad (6)$$

In the equation, g(κ) is the complex type two-dimensional Gaussian random white noise; and q is the calibration vector. With respect to isotropic turbulence, $\Phi_n(\vec{\kappa})$ and $\Delta\Phi(r)$ rely only on $|\vec{\kappa}|$ and $|r|$. Therefore, only if the density function Φ_n of the refractivity fluctuation spectrum is given, the phase fluctuation ΔΦ(r) can be obtained by using Eq. (6). However, we know that the turbulence spectrum is very wide in scope, within the range $2\Pi/L_0$ and $2\Pi/l_0$, the turbulence seriously affects laser transmission. If the Cauchy 2 fast Fourier transform algorithm is used for numerical calculation on Eq. (6), in order to attain the required calculated sampling density ($\Delta\kappa=2\Pi/L_0$) or $\Delta x=l_0$; usually, l_0 is in millimeters, and L_0 is approximately 10 or more meters, the divergent dot-matrix number of the phase screen will attain 8192x8192. However, the numerical calculated dot matrix number in the transmission equation is only a small part of them. We can see that this is very uneconomical for the traditional divergence calculation method corresponding to the space and

Fourier spectrum domain dot-matrix number. Moreover, it is very difficult to have this much computer memory and computational volume. Thus, many authors sacrifice the accuracy (reducing the dot matrix number) to upgrade the computing speed and reduce the internal memory [2,3].

III. Folding FFT Algorithm

We cite an example with twice-folding to discuss the algorithm in Eq. (6). If the number of space divergent points is 2Nx2N and the sample interval is Δx then the divergent points of the Fourier spectral domain are 2Nx2N, $\Delta\kappa = 2\Pi/N\Delta x$. After divergence of Eq. (9), we have:

$$\Delta\varphi(m,n) = \sum_{n'=-N}^{N-1} \sum_{m'=-N}^{N-1} f(m',n') \exp[i2\pi(nn'+mm')/N] \tag{7}$$

In the equation, $f(m',n') = \frac{2\pi}{L} g(m',n') F_{\varphi}^{1/2}(m',n')$, $L = N\Delta x$ is the overall width of the space sample. The scalar factor $q = \Delta\kappa^{-1}$. Let us rewrite Eq. (7) to become:

$$\Delta\varphi(m,n) = \sum_{n'=-N}^{N-1} \exp(i2\pi nn'/N) \Big[\sum_{m'=-N}^{N-1} f(m_1', n') \exp(i2\pi m_1' m/N) + \sum_{m'=0}^{N-1} f(m',n') \exp(i2\pi m' m/N) \Big] \tag{8a}$$

Let $m_1' = m' - N$, and applying the periodicity of the trigonometric function, we obtain

$$\Delta\varphi(m,n) = \sum_{m'=0}^{N-1} \exp(i2\pi mm'/N) \Big\{ \sum_{m'=-N}^{N-1} [f(m'-N,n') + f(m',n')] \cdot \exp(i2\pi m'/N) \Big\} \tag{8b}$$

Similarly, by conducting a transform on the summation equation of

n', finally we obtain:

$$\Delta\varphi(m,n)=\sum_{m'=0}^{N-1}\sum_{n'=0}^{N-1} f(m'-N,n'-N)+f(m'-N,n') +f(m',n'-N)+f(m',n')]\exp[i2\pi(m'm+n'n/N] \qquad (8c)$$

Obviously, only NxN fast Fourier transforms are required for computing Eq. (8c); the maximum sampling frequency is $2\Pi/\Delta x$. We compare the folding FFT algorithm with the conventional algorithm and discover the following: by one-to-one correspondence of the number of points in the space and frequency domains in the conventional algorithm, if the space frequency is of the same height for sampling, the dot matrix number should be $N_1xN_1=2Nx2N$. In other words, 2Nx2N fast Fourier transforms should be conducted, and the number of multiplications is [7]:

$\frac{1}{2}N_1^2(r+1)=2N^2(r+1)$, $N=2^\gamma$; γ is a positive integer. The number of summations is $N^2_1(r+1)=4N^2(r+1)$. The number of multiplications in the folding algorithm is $(1/2)N^2r$ and the number of summations is $N^2(r+4)$. Thus we know the number of multiplications in the folding FFT algorithm is one-quarter that of the conventional algorithm, and the number of summations is also greatly reduced. Correspondingly, the computer internal memory required is only one-quarter as under the conventional algorithm. In the conventional algorithm, if the NxN dot matrix number is used, the sampling highest space frequency is $2p/2\Delta x$, which is one-half as under the folding algorithm; thus, the computational accuracy will be greatly reduced. Besides, we can see in the above-

mentioned operations, in principle, more than twice-folding computations can be conducted to further upgrade the sampling accuracy of the turbulence density spectrum. In short, with the same sampling frequency (that is, the same computational accuracy) the folding FFT algorithm is better than the conventional algorithm with respect to computing speed and the internal computer memory required.

IV. Numerical Computational Results and Discussion

We applied the twice-folding FFT algorithm to conduct numerical simulation on the equivalent-level homogeneous atmospheric transmission of a collimated gaussian laser beam; the refractivity fluctuation spectrum applies the Von Karman function. The sampling total width L=2.56m, N=128, L_0=62.8m, λ=1.0μm, Δz=100m, at the 1/e power point of the gaussian light beam, the beam waist radius a_0=0.5m, and the structure constant C_n^2 of the turbulence refractivity is 10^{-16} to 10^{-12} $m^{-2/3}$. Corresponding to weak and strong turbulence features, the maximum transmission distance is 10km. Fig. 1a is an example of phase screen. We can see that there are obvious indications in the phase screen from small-scale phase fluctuation to large-scale phase tilt. Fig. 1b shows a comparison with the theoretical results and the phase screen reconstruction phase structure function D(r). The "+" indicates the average results of ten phase screens; the solid curve shows the theoretical results. Their agreement indicates a great improvement over the results in

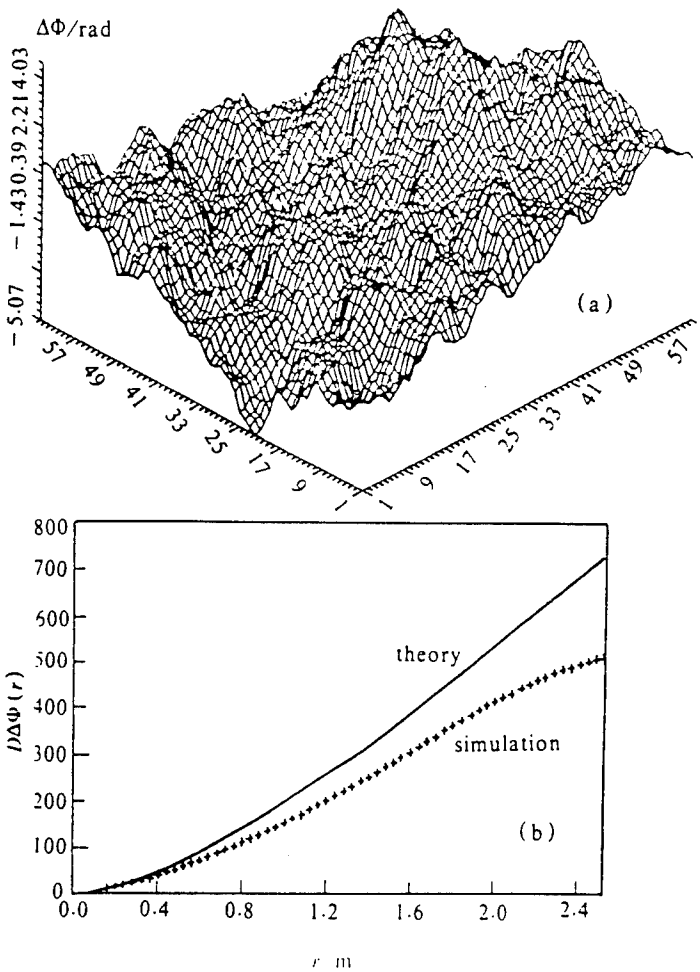

Fig. 1 (a) An example of phase screen [Horizontal axis drawn with 2 points interval on (x, y) grid]
(b) Phase structure function. r distance of 2 points on grid

[1]. This indicates that the structure functions in the conventional algorithm gradually decreases and approaches zero with the greater intervals r. The results are quite different from the theoretical results of $r^{5/3}$.

Fig. 2 shows an example of intensity distribution on a light beam cross section at 10km. a is the three-dimensional display and b is the intensity isopleth. From the figure we can see very

strong scintillation and light beam expansion effects.

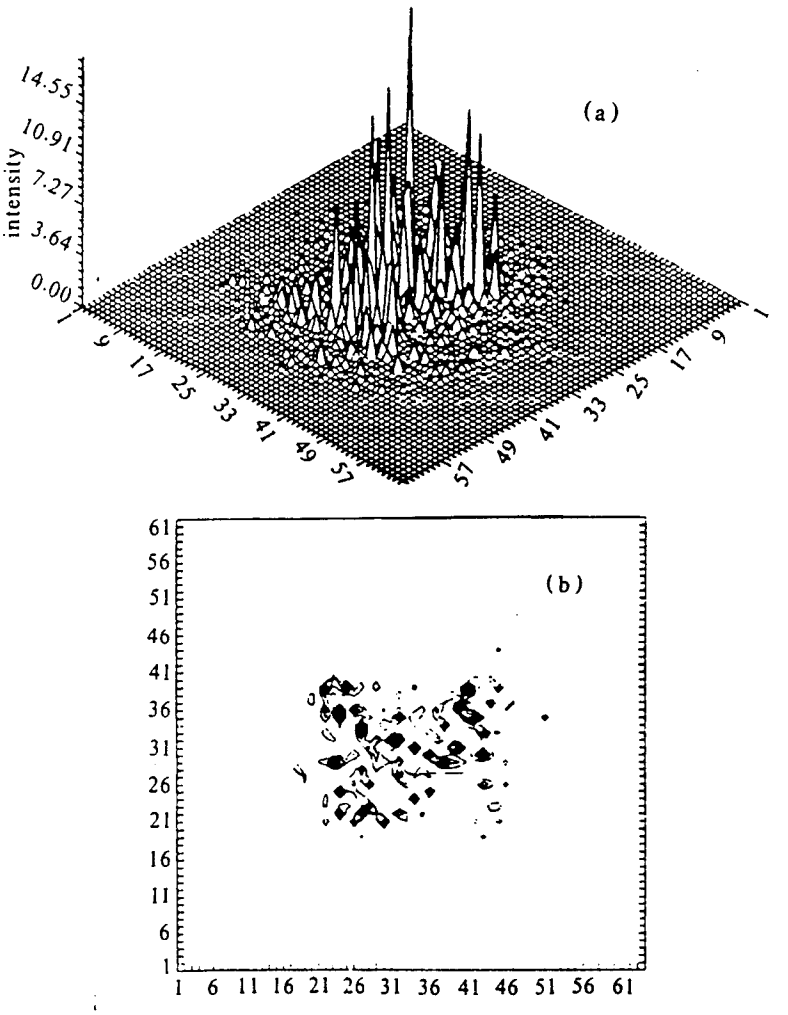

Fig. 2 An example of laser intensity distribution at z = 10km, $C_n^2 = 10^{-14} m^{-2/3}$
[Horizontal axis drawn with 2 points interval on (x, y) grid]
(a) 3D view, (b) Isoplath [intensity interval 1.0]

Fig. 3a is the normalized variance σ_I^2 of the light intensity scintillation varying with transmission distance. The "+" indicates the numerical simulation result; the solid curve shows the theoretical results. In the weak scintillation region,

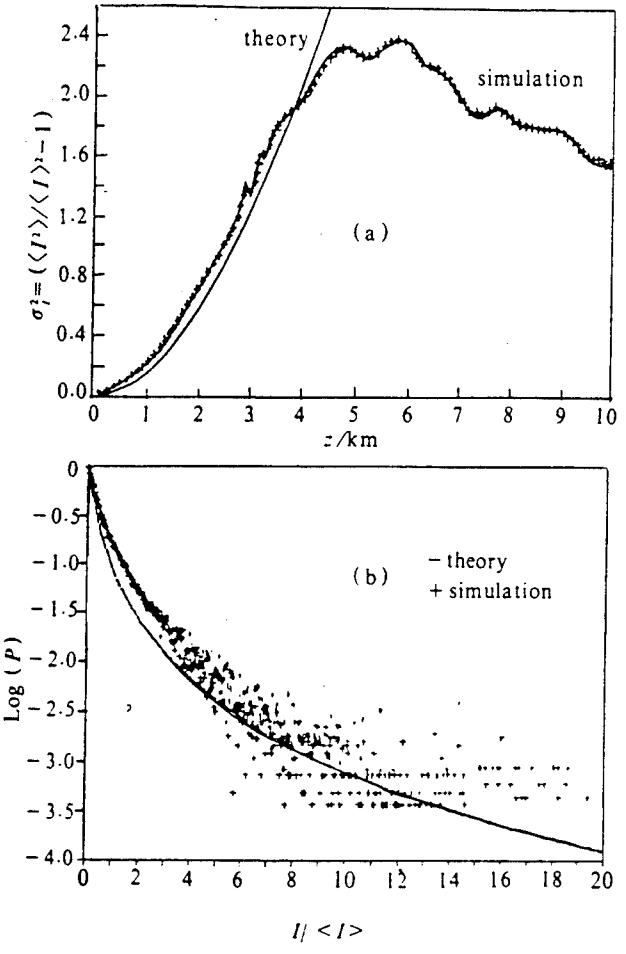

Fig. 3 (a) Normalized intensity deviation square *vs* propagation distance
(b) Probability of intensity scintilation, $\sigma_I^2 = 2.4$

σ_1^2 is proportional to β_0^2 ($\beta_0^2 = 1.23 C_n^2 k^{7/6} z^{11/6}$) [8], which is consistent with the theoretical results. When the light transmits to a certain distance, $r_0^2/\lambda z = 1$ is the turbulence perturbation Rayleigh distance, and light intensity simulation is at saturation. Then σ_1^2 decreases with a certain slope with increase in β_0^2. This result also agrees with the theoretical estimate [8]. Fig. 3b shows the probability distribution of

light intensity scintillation. I is light intensity; <I> is average light intensity; and the statistical region radius is a_0. The "+" indicates the numerical simulation result; the solid curve is the distribution of positive theoretical logarithms [9]. Both are also quite close. In the situation of greater I/<I>, the numerical simulation results have greater divergence. This is because the greater the I/<I>, the smaller is the probability. Thus, the statistical number of points is also smaller. With respect to the numerical simulation of light intensity scintillation, previously no research reports had been published. This is possibly due to the fact of low sampling density and a small number of high-frequency components of the structure phase screen, thus neglecting the effect on light intensity scintillation due to high-frequency spectral turbulence, so that it is difficult to obtain better results.

Generally, the Strehl ratio is adopted in evaluating light beam quality during laser beam transmission in a turbulent atmosphere. Fig. 4 shows the variation of Strehl ratio with D/r_0 for the collimated gaussian light beam transmitted in a turbulent atmosphere. We use $D=2\sqrt{2}\,a_0$. r_0 varies with C_n^2 and transmission distance z. The "□" in the numerical simulation results also agrees considerably with the solid curves [10].

As mentioned above, in the authors' view, this computational mode more truly, overall, reflects the effect on laser beam transmission by atmospheric turbulence because whatever the light intensity scintillation or the light-beam quality Strehl ratio,

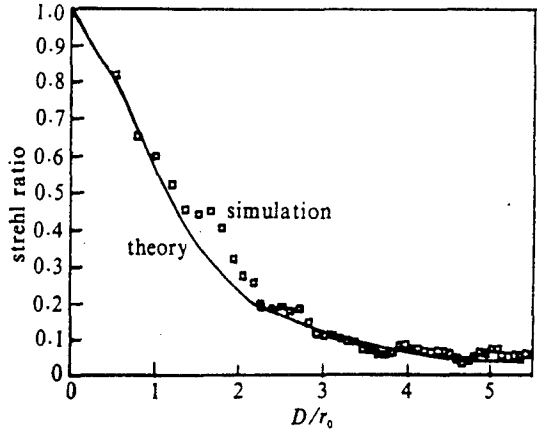

Fig. 4 Variation of the Strehl ratio with D/r_0

the comprehensive effect is imposed on turbulence from all frequency ranges (large and small scales).

V. Conclusions

In the folding FFT algorithm proposed by the authors, there is an improvement in the conventional numerical computation of laser transmission in a turbulent atmosphere. The folding algorithm has higher computational accuracy and speed, and lower requirements for internal computer memory. To invert a phase screen on a VAX-II, 7min is required under the conventional algorithm, but only a little more than 3min with the folding FFT algorithm. This will have a great effect on the atmospheric transmission of a high-powered laser (especially when considering the interaction between thermal blooming and turbulence), and the establishment of a four-dimensional numerical computational

program. Twice-folding can yield satisfactory results. Actually, the folding FFT algorithm can be used not only in numerical simulation of laser transmission in the atmosphere, but also it is useful in computing the number of sampling points in the frequency-domain that requires a much larger number of sampling points in the space domain, or vice versa.

The authors express their gratitude to comrade Wang Ningquan because of his help in preparing the figures and tables.

The first draft of the article was received on December 28, 1991; the final revised draft was received for publication on July 28, 1992.

REFERENCES

[1] Hermah B J et al, *SPIE. proc* OEI laser'90, **1221**:183.
[2] Martin J M et al. *Appl Opt* 1988, **27** (11):2111.
[3] Knepp D L *Proc IEEE*, 1983, **71** (6):722.
[4] Fleck J A et al. *Appl Phys*, 1976, **10** (2):129.
[5] Tataski B N. 湍流大气中的波传播理论 (中译文), 北京:科学出版社, 1978.
[6] Strohbehn.J W, Laser Beam Propagation in the Atmosphere.*Topics in Appl Phys*. **25**.
[7] 布赖姆 E O. 快速付里叶变换, 上海:上海科技出版社, 1979.
[8] Zuev B E. 激光大气传播. 中国工程物理研究院译, 1990.
[9] 宋正方, 应用大气光学基础. 气象出版社, 1990.
[10] Valley G C. *Appl Opt*, 1979, **18** (6):984.

RECENT ADVANCES IN BEAM TRANSFORMATION OPTICS PART I: DIFFRACTION THEORY IN THE TIME-SPACE DOMAINS AND OPERATOR METHODS

Lu Baida, Cai Bangwei, Zhang Bin,
Feng Guoying, and Dong Ming

Department of Optoelectronic Science and Technology
Sichuan University, Chengdu 610064

ABSTRACT The purpose of this monograph, which is divided into two parts, is to give a general review for the recent advances in beam transformation optics, including some results obtained by our group. Part I deals with the diffraction theory in the time−space domains and operator optical methods, as well as their applications to laser optics and high power laser technology.
KEY WORDS beam transformation, high power laser technology, diffraction integrals in the time−space domains, operator optical methods.

I. Introduction

In the research scene dealing with laser beams passing through optical elements and systems (including optical resonator) with the transmission transformation rule and the control of light beam quality, light beam transformation optics (also referred as to as laser optics) has seen rapid development of late owing to advances in laser science and technology, especially high-powered laser technology. Some new research directions have appeared. There are many papers and research

reports in China and abroad on this field. In reference [1], the authors discussed some fundamental analytical methods and applications on beam transformation optics. In this paper, by including the related problem of high-powered laser technology, more detailed descriptions are given on the advances in beam transformation optics. This paper is divided into two parts. Part I discusses diffraction theory, Hamiltonian optics, and operator methods in the time-space domain. Part II describes the matrix optical method and Lie algebraic theory. Finally, a brief analysis is made on the correlated problems on the internal relationship in the theory and high-powered laser technology. The paper emphasizes the explanation of physical concepts and methods. Some application examples cited also serve this purpose. Further understanding about details and actual applications can be found in the references.

II. Diffraction Theory in the Space-time Domain

2.1. Kirchhoff and Wickens-Fennell diffraction integral

As is well-known, the fundamental formula describing the scalar diffraction field is [2]

$$U_2(x_2, y_2) = \left(-\frac{i}{\lambda}\right) \iint_S U_1(x_1, y_1) \frac{e^{ikr}}{r} \left(\frac{1+\cos\alpha}{2}\right) dx_1\, dy_1 \qquad (2.1)$$

In the equation, $U_1(x_1, y_1)$ and $U_2(x_2, y_2)$ are, respectively, the field oscillation amplitudes at the point of origin and the field point; r is the spacing between the point of origin and the field

point. (1+cosα)/2 is called the tilt factor; α is the angle of intersection between the normal line at the point (x1,y1) on the S-plane and ρ; λ and k are, respectively, the wavelength and wave number. The integration is performed on the S-plane. Generally, Eq. (2.1) is called the Kirchhoff diffraction formula.

When the Fennell approximation is established, in other words, the distance L between the diffraction plane and the observation plane is much greater than the diffraction aperture and the linearity in the observation region

$$\rho \approx L, \cos\theta \approx 1 \quad \text{(that is, } L \gg |x_2 - x_1|, |y_2 - y_1| \text{)} \quad (2.2)$$

Eq. (2.1) is converted into the Wickens-Fennell diffraction integral.

$$U_2(x_2, y_2) = (-\frac{i}{\lambda L}) e^{ikL} \iint_S U_1(x_1, y_1) \exp\{ \frac{ik}{2L} [(x_2 - x_1)^2 + (y_2 - y_1)^2] \} dx_1 dy_1 \quad (2.3)$$

If we further increase L so that the following equation is satisfied

$$L \gg \frac{k}{2} (x_1^2 + y_1^2)_{max} \quad (2.4)$$

Then Eq. (2.3) is simplified as the Fraunhofer diffraction integral

$$U_2(x_2, y_2) = (-\frac{i}{\lambda L}) e^{ikL} - \exp[i \frac{k}{2L} (x_2^2 + y_2^2)] \iint_S U_1(x_1, y_1) \exp[-\frac{ik}{L} (x_1 x_2 + y_1 y_2)^2] \, dx_1 \, dy_1 \quad (2.5)$$

This is easier than Eq. (2.3) for solving by computer. With respect to the diffraction problem, of large space domain in classical optics, Eq. (2.3) is suitable; the equation can also be used in studying that the free space exists between the diffraction plane and the observation plane, such as transmission

and phase control problems of a laser beam in the atmosphere when such effects as the following are neglected: nonlinearity effect, observation and linear scattering. For a long time, researchers thought that Eq. (2.3) was universally established; however, advances in laser technology raise a challenge to this viewpoint. The related research mainly includes two aspects. First, recalling the original Kirchhoff formula, study the gaussian laser beam without side axes, or light beam of random wavefront passing through an asymmetrical medium, in addition to diffraction by a diaphragm of arbitrary shape [3,4]. Second, Eq. (2.3) is generalized to deal with such problems, including the diffraction problem of the space domain of a complex optical system, which is Collins' formula [5]. Thus, further expand the equation to study the more general time-space domain diffraction [6]. In the following, the latter problem is emphasized in the discussion.

2.2. Time-space domain diffraction integral

Recently, Kostenbauder proved [6] that the Wickens-Fennell diffraction integration form, in the broad sense (including the time variable) (t, f = frequency) and space variable (x, θ) is

$$U_2(x_2,t_2)=\eta\iint U_1(x_1,t_1)\exp\left[-\frac{i\pi}{\lambda_0}\begin{pmatrix}x_1\\x_2\\t_1-t_2\end{pmatrix}^{T}\begin{pmatrix}\alpha&\beta&\gamma\\\beta&\delta&\varepsilon\\\gamma&\varepsilon&\zeta\end{pmatrix}\begin{pmatrix}x_1\\x_2\\t_1-t_2\end{pmatrix}\right]dx_1\,dt_1 \quad (2.6)$$

In the equation, the $\begin{pmatrix}\alpha&\beta&\gamma\\\beta&\delta&\varepsilon\\\gamma&\varepsilon&\zeta\end{pmatrix}$ matrix (describing the light beam transmission)

$$\begin{pmatrix} x \\ t \\ \theta \\ \lambda_0 f \end{pmatrix}_2 = \begin{bmatrix} A & 0 & B & E/\lambda_0 \\ G & 1 & H & I/\lambda_0 \\ C & 0 & D & F/\lambda_0 \\ 0 & 0 & 0 & 1 \end{bmatrix} \begin{pmatrix} x \\ t \\ \theta \\ \lambda_0 f \end{pmatrix}_1 = \begin{pmatrix} \mathbf{A} & \mathbf{C} \\ & \\ \mathbf{B} & \mathbf{D} \end{pmatrix} \begin{pmatrix} x \\ t \\ \theta \\ \lambda_0 f \end{pmatrix}_1 \tag{2.7}$$

There exists the relationship

$$\alpha = \frac{\lambda_0 A(EH-BI)+E^2}{\lambda_0 B(EH-BI)}, \quad \beta = \frac{I}{EH-BI}, \gamma = \frac{E}{EH-BI},$$
$$\delta = \frac{D(EH-BI)+\lambda_0 H^2}{B(EH-BI)}, \varepsilon = \frac{\lambda_0 H}{EH-BI}, \zeta = \frac{\lambda_0 B}{EH-BI} \tag{2.8}$$

The integration constant is

$$\eta = i/\sqrt{\lambda_0 (EH-BI)} \tag{2.9}$$

$\boldsymbol{\lambda_0}$ is the reference pulse wavelength. At the upper corner, "T" is the transpose operator. Eq. (2.6) is a relatively universal formula, which unifiedly describes an optical system when passing through the time-space transformation matrix $\begin{pmatrix} A & C \\ B & D \end{pmatrix}$ the variation of time-space parameters for the light beam. Further research is worthwhile. We should take note that Eqs. (2.6) and (2.7) are derived with respect to the axisymmetric optical system. With respect to a nonaxisymmetric system, the matrix $\begin{pmatrix} x \\ t \\ \theta \\ \lambda_0 f \end{pmatrix}$ in Eq. (2.7) should be replaced with

the matrix $\begin{pmatrix} x \\ y \\ t \\ \theta \\ \varphi \\ \lambda_0 f \end{pmatrix}$. In the equation, the 4x4 matrix should be expanded into a 6x6 matrix. Eq. (2.6) should also be correspondingly expanded.

2.3. Collins' formula

When discussing only the space diffraction problem, Eq. (2.6) is simplified as

$$U_2(x_2) = \sqrt{\frac{i}{\lambda_0 B}}\, e^{-ikL} \int U_1(x_1) \exp[-\frac{ik}{2B}(Ax_1^2 - 2x_1x_2 + Dx_1^2)]\, dx_1 \quad (2.10a)$$

$$(B \neq 0)$$

$$U_2(x_2) = \frac{1}{\sqrt{A}}\, e^{-ikL} \int \exp(-\frac{ikC}{2A} x_2^2)\, U_1(\frac{x_2}{A}), \quad (B=0) \quad (2.10b)$$

In the equations, A, B, C, D are elements in the following transformation matrix

$$\begin{pmatrix} x_2 \\ \theta_2 \end{pmatrix} = \begin{pmatrix} A & B \\ C & D \end{pmatrix} \begin{pmatrix} x_1 \\ \theta_1 \end{pmatrix} \quad (2.11)$$

Eq. (2.10) is the well-known Collins' formula, which can be used to study the transformation problem of complex optical systems in which a laser beam passes through a transformation matrix $\begin{pmatrix} A & B \\ C & D \end{pmatrix}$, and also can be used to the motion rule [7] of laser beam in an optical resonator. In addition, well-known interference and diffraction phenomena in classical optics can also be unifiedly processed with Eqs. (2.10a) and (2.10b).

2.4. Time-domain diffraction integral

Now the transmission problem of dispersion optical pulses is studied. Here the time-space domain diffraction integral, Eq. (2.6), is transformed into the time domain diffraction integral

$$U_2(\tau_2)=\sqrt{-\frac{i\omega_0}{2\pi B}}\ e^{i\omega_0\xi_0}\int U_1(\tau_1)\exp[\frac{i\omega_0}{2B}\ (A\tau_1^2-2\tau_1\tau_2+D\tau_2^2)]d\tau_1\ ,(B\neq 0) \quad (2.12a)$$

$$U_2(\tau_2)=\frac{1}{\sqrt{A}}\ e^{i\omega_0\xi_0}\exp(\frac{i\omega_0}{2A}\ C\tau_2^2)U_1(\frac{\tau_2}{A}\ ),(B=0) \quad (2.12b)$$

In the equations

$$\tau=t-\beta'(\omega_0)z=t-\frac{z}{v_g}\ ,\ \ \xi=\omega_0\beta''(\omega_0)z \quad (2.13)$$

v_g is the group velocity; ß" describes the dispersion of group velocity; ω_0 is the center frequency of the dispersion pulse, however

$$\begin{pmatrix}\tau_2\\ \frac{d\tau_2}{d\xi}\end{pmatrix}=\begin{pmatrix}A & B\\ C & D\end{pmatrix}\begin{pmatrix}\tau_1\\ \frac{d\tau_1}{d\xi}\end{pmatrix} \quad (2.14)$$

Obviously, Eq. (2.12) can be readily derived from Eq. (2.10) with the following time-space variable analogy [9,10]:

$$\omega_0\beta''z=\xi\longleftrightarrow z\ ,\ t-\beta'z=\tau\longleftrightarrow x,\ \omega_0\longleftrightarrow -k \quad (2.15)$$

More rigorously, proof should be exercised, beginning from the time domain dispersion wave motion equation [11]. Take note, similarly as in the classical optics situation, for sake of convenience in studying the problem, that there are two kinds of equivalence symbol utilization formulas in Eqs. (2.7), (2.8), and

(2.12). For example, another equivalence form of Eq. (2.12a) is

$$U_2(\tau_2)=\sqrt{\frac{i\omega_0}{2\pi B}}\,e^{-i\omega_0\xi_0}\int U_1(\tau_1)\exp[-\frac{i\omega_0}{2B}(A\tau_1^2-2\tau_1\tau_2+D\tau_2^2)]d\tau_1\ ,(B\neq 0) \qquad (2.16)$$

III. Hamiltonian Optics

Another route in studying light beam transformation is to try to include the movement rule of the light frequency electromagnetic field into the framework of unified theory of physics. Thus, the matured physical equations and the related mathematical means in research can be directly used to deal with problems of laser optics. Here, analogy and inference are methods in scientific research with another successful example. First, let us recall Fermat's principle, which explains that the variation is zero along the real optical path of the light rays. In other words,

$$\delta\int n(x,y,z)dl=0 \qquad (3.1)$$

In the equation, n is the refractivity of the medium. Obviously, Eq. (3.1) is similar in form to the Hamiltonian principle in analytical mechanics. Next, the Helmholtz equation can be directly derived from Maxwell's equations:

$$\nabla^2 U+k^2 U=0 \qquad (3.2)$$

with side axis approximation, the equation is transformed to become [12]

$$\frac{\partial^2 U}{\partial x^2}+\frac{\partial^2 U}{\partial y^2}-2ik\frac{\partial U}{\partial z}=0 \qquad (3.3)$$

Eq. (3.3) is generally referred to as the equation similar to the Schroedinger wave equation, with similar forms as the Schroedinger equation well-known in quantum mechanics. Therefore, physicists well acquainted with classical mechanics and wave motion mechanics will very easily adopted the analogical approach in setting up Hamiltonian optics [13, 14] and operator optics, with elaboration. In Hamiltonian optics, there are the following most important results:

3.1. Optical regular variable and operator form

The positional direction of a light beam on a transverse plane can be written as the following equation by using the regular coordinates q_x and q_y and the regular momenta p_x and p_y.

$$q_x = x \ , \ q_y = y, \ p_x = \frac{n\frac{dx}{dz}}{\sqrt{1+(\frac{dx}{dz})^2+(\frac{dy}{dz})^2}} \ , \ p_y = \frac{n\frac{dy}{dz}}{\sqrt{1+(\frac{dx}{dz})^2+(\frac{dy}{dz})^2}} \qquad (3.4)$$

In the side axis approximation, there is

$$p_x = n\frac{dx}{dz} = n\theta, p_y = n\frac{dy}{dz} = n\varphi \qquad (3.5)$$

The corresponding regular conjugate operator is

$$\hat{q}_x = \hat{x}, \ \hat{q}_y = \hat{y}, \ \hat{p}_x = -ik^{-1}\frac{\partial}{\partial x} \ , \ \hat{p}_y = -ik^{-1}\frac{\partial}{\partial y} \qquad (3.6)$$

3.2. Optical Lagrangian equation

$$\begin{cases} \dfrac{d}{dz}\left(\dfrac{\partial L}{\partial\left(\dfrac{dx}{dz}\right)}\right)=\dfrac{\partial L}{\partial x} \\ \dfrac{d}{dz}\left(\dfrac{\partial L}{\partial\left(\dfrac{dy}{dz}\right)}\right)=\dfrac{\partial L}{\partial y} \end{cases} \tag{3.7}$$

In the equation, the optical Lagrangian argument is

$$L=n(x,y,z)\sqrt{1+\left(\frac{dx}{dz}\right)^2+\left(\frac{dy}{dz}\right)^2} \tag{3.8}$$

3.3. Optical Hamiltonian Regular Equation

$$\begin{cases} \dfrac{\partial H}{\partial x}=-\dfrac{dp_x}{dz} \\ \dfrac{\partial H}{\partial y}=-\dfrac{dp_y}{dz} \\ \dfrac{\partial H}{\partial p_x}=\dfrac{dx}{dz} \\ \dfrac{\partial H}{\partial p_y}=\dfrac{dy}{dz} \end{cases} \tag{3.9}$$

Optical Hamiltonian argument:

$$H=-[\,n^2(x,y,z)-p_x^2-p_y^2\,]^{1/2} \tag{3.10}$$

By using the analogical method, the following useful conclusions can be obtained: (1) as is well known, when $\hbar$ =h/2Π (h is Planck's constant) --->0, the results in quantum mechanics are consistent with the results in classical mechanics. Upon analogy, when k^{-1} --->0 (short wavelength approximation), the transition from wave motion optics to light ray optics is

executed. (2) With the principle of indeterminacy in quantum mechanics,

$$\Delta x \Delta p_x \geq \hbar/2 \tag{3.11}$$

(Δx and Δp are, respectively, the coordinate and momentum indeterminates) with analogy, in laser optics there is [12]

$$\theta_m W_{0m} \geq M^2 \frac{\lambda}{\pi} \tag{3.12}$$

In the equation, θ_m and W_{0m} are, respectively, the far-field divergence angle and the light beam waist dimension of the laser light beam with mode sequence number m; m^2 is the correlated factor of the light mode (referred to as the M^2-vector). Only for a gaussian light beam of ideal fundamental mode (m=0), there is

$$\theta_0 W_0 = \frac{\lambda}{\pi} \tag{3.13}$$

Eqs. (3.12) and (3.13) explain that small light beam divergence and small light beam waist dimension are unable to be realized at the same time; this is the fundamental relationship equation in controlling light beam quality. Eq. (3) marks the derivation of the quantum-mechanical formula system by using operators as the mechanical quantity. On analogy, the operator method can be conveniently used to deal with the light beam transmission transformation with diffraction effect for development, thus performing the operator optics.

IV. Operator Optical Method

Operator optics is expressed by a method proposed and developed by Nazarathy and Shamir et al. [15, 16]. In the

expression method, expression with a regular operator is more complete. The nonregular operator method is still under development [17].

4.1. Fundamental regular operator and operator form in Collins' formula

Let us assume that u(x) is a random function. From Eq. (3.6), we have

$$\begin{aligned} \hat{x}u(x) &= x\,u(x) \\ \hat{p}_x u(x) &= -ik^{-1}\frac{\partial u(x)}{\partial x} \end{aligned} \tag{4.1}$$

and

$$[\hat{x}, \hat{p}_x] = \hat{x}\,\hat{p}_x - \hat{p}_x\,\hat{x} = ik^{-1} \tag{4.2}$$

Define the regular transformation operator T, which satisfies (for convenience in writing, the subscript x is omitted in p_x in the following):

$$\begin{aligned} \hat{x}_2 &= D\hat{x}_1 - B\hat{p}_1 \\ \hat{p}_2 &= -C\hat{x}_1 + A\hat{p}_1 \end{aligned} \tag{4.3}$$

In the equation, A, B, C, and D from

$$\begin{pmatrix} x_2 \\ p_2 \end{pmatrix} = \begin{pmatrix} A & B \\ C & D \end{pmatrix} \begin{pmatrix} x_1 \\ p_1 \end{pmatrix} = M \begin{pmatrix} x_1 \\ p_1 \end{pmatrix} \tag{4.4}$$

are the M elements of the transformation matrix in the expression.

It is easy to prove that T satisfies

$$T[M_2]\mathrm{T}[M_1] = \pm \mathrm{T}[M_2 M_1] \tag{4.5}$$

$$\{\mathrm{T}[M_3]\mathrm{T}[M_2]\}\mathrm{T}[M_1] = \mathrm{T}[M_3]\{[M_2]\mathrm{T}[M_1]\} \tag{4.6}$$

$$\{T[M]\}^{-1} = T[M^{-1}] \tag{4.7}$$

$$T[E] = 1 \quad (\text{式中}, E = \begin{pmatrix} 1 & 0 \\ 0 & 1 \end{pmatrix}) \tag{4.8}$$

Therefore, the regular operators T constitute a group. Actually, T is part of the Metaplectic group, isomorphous with the Symplectic group.

In the following, the fundamental regular operators can be expressed in terms of T as

(1) Square phase operator

$$Q[\alpha] = \exp(\frac{ik}{2}\alpha x^2) = T\begin{bmatrix} 1 & 0 \\ \alpha & 1 \end{bmatrix} \tag{4.9}$$

(2) Scale operator

$$V[\beta]u(x) = T\begin{bmatrix} \beta^{-1} & 0 \\ 0 & \beta \end{bmatrix} u(x) = \beta^{1/2} u(\beta x) \tag{4.10}$$

(3) Fourier transform operator

$$F = (i\lambda_0)^{-1/2}\int_{-\infty}^{+\infty} dx_1 \exp(-ikx_1 x)\cdots = T\begin{bmatrix} 0 & 1 \\ -1 & 0 \end{bmatrix} \tag{4.11}$$

(4) Fennell free-space transmission operator

$$R[\gamma] = \exp(-\frac{ik}{2}\gamma p^2) = T\begin{bmatrix} 1 & \gamma \\ 0 & 1 \end{bmatrix} \tag{4.12}$$

By using Eqs. (4.9) to (4.12), as well as the related computation equations, Collins' formula (Eq. (2.10)) can be written as (neglecting the nonessential phase factor e^{ikl}, hereinafter)

$$U_2(x_2) = Q[D/B]V[1/B]FQ[A/B]U_1(x_1), \ (B \neq 0) \tag{4.13a}$$

$$U_2(x_2) = Q[C/A]V[1/A]U_1(x_2), \ (B = 0) \tag{4.13b}$$

4.2. Applications of special optical system

By using the fundamental regular operators, it is easy to simplify the commonly-seen optical systems in physics and optics, such as:

(1) Fourier transform system

$$T\begin{bmatrix} 0 & B \\ -B^{-1} & D \end{bmatrix} = Q[\frac{D}{B}]V[\frac{1}{B}]F \tag{4.14}$$

(2) imaging system

$$T\begin{bmatrix} A & 0 \\ C & A^{-1} \end{bmatrix} = Q[\frac{C}{A}]V[\frac{1}{A}] \tag{4.15}$$

(3) remote focus system

$$T\begin{bmatrix} D^{-1} & B \\ 0 & D \end{bmatrix} = R[\frac{B}{D}]V[D] \tag{4.16}$$

(4) Fennell transform system

$$T\begin{bmatrix} A & B \\ -B^{-1} & 0 \end{bmatrix} = V[\frac{1}{B}]FQ[\frac{A}{B}] \tag{4.17}$$

(5) ideal amplifier

$$T\begin{bmatrix} A & 0 \\ 0 & A^{-1} \end{bmatrix} = V[\frac{1}{A}] \tag{4.18}$$

(6) ideal spectrum analysis instrument

$$T\begin{bmatrix} 0 & B \\ -B^{-1} & 0 \end{bmatrix} = V[\frac{1}{B}]F \tag{4.19}$$

4.3. Misalignment optical system

Let us assume that a transformation matrix is the optical system of $\begin{pmatrix} A & B \\ C & D \end{pmatrix}$. Relative to the position and direction of

the ideal optical axis, the misalignments are, respectively, μ_x and μ_p (as shown in Fig. 1). the misalignment vector is

$$\mu = \begin{pmatrix} \mu_x \\ \mu_p \end{pmatrix} \tag{4.20}$$

By introducing the linear phase alignment G and the drift operator S [18]

$$G[\delta]u(x) = e^{ik\delta x}u(x) \tag{4.21}$$

$$S[m]u(x) = u(x-m) \tag{4.22}$$

the misalignment operator

$$W[\mu] = W\begin{bmatrix} \mu_x \\ \mu_p \end{bmatrix} = G[-\mu_p]\, S[-\mu_x] \tag{4.23}$$

The Heisenberg-Weyl transform operator

$$\hat{W}[\mu, l] = \exp[ik(l + \frac{1}{2}\mu_x\mu_p)]S[-\mu_x]G[-\mu_p] \tag{4.24}$$

and the augmented matrix

$$A = \left(\begin{array}{cc|c} M & & \varepsilon \\ 0 & 0 & 1 \end{array}\right) = \begin{pmatrix} A & B & E \\ C & D & F \\ 0 & 0 & 1 \end{pmatrix} \tag{4.25}$$

Later, by using the operator commutation equation, the misalignment transformation operator

$$H = W^{-1}[\mu_1]T[M]W[\mu_2] \tag{4.26}$$

can be written as [19]

$$\begin{aligned} H &= T\left[\left(\begin{array}{cc|c} 1 & & -\mu_2 \\ 0 & 0 & 1 \end{array}\right), \frac{1}{2}\mu_{2x}\mu_{2p}\right] T\left[\left(\begin{array}{cc|c} M & & 0 \\ 0 & 0 & 1 \end{array}\right), 0\right] T\left[\left(\begin{array}{cc|c} 1 & & \mu_1 \\ 0 & 0 & 1 \end{array}\right), \frac{1}{2}\mu_{1x}\mu_{1p}\right] \\ &= T[A, L] \end{aligned} \tag{4.27}$$

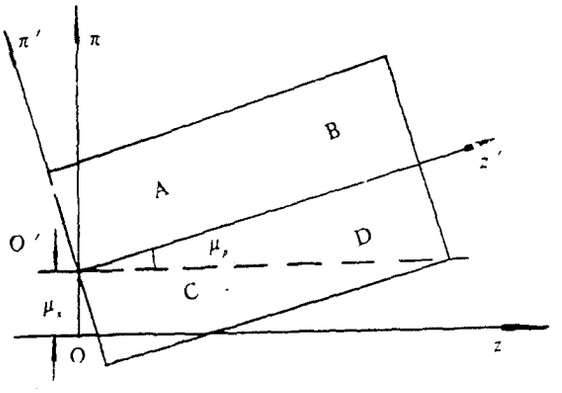

Fig. 1 A misalignment optical system

In the equation, the total augmented matrix is

$$A=\left(\begin{array}{cc|c}1 & & -\mu_2 \\ 0 & 0 & 1\end{array}\right)\left(\begin{array}{cc|c}\mathrm{M} & & 0 \\ 0 & 0 & 1\end{array}\right)\left(\begin{array}{cc|c}1 & & \mu_1 \\ 0 & 0 & 1\end{array}\right)=\left(\begin{array}{cc|c}\mathrm{M} & & \mathrm{M}\mu_1-\mu_2 \\ 0 & 0 & 1\end{array}\right) \quad (4.28)$$

the phase drift factor is

$$\mathrm{L}=\frac{1}{2}\left(\mu_{2x}\mu_{2p}+\mu_{1x}\mu_{1p}\right)+\frac{\mu_2}{k}\times\mathrm{M}\mu_1 \quad (4.29)$$

Up to now, great successes have been obtained by using the regular operator expression method to deal with problems of coaxial and misalignment optical systems, physical optics, Fourier optics, and optical resonators. A shortcoming is the fact that the "aperture factor" A is used to express the diaphragm of the hard-edged small aperture. This aspect needs further study.

4.4. Regular operator expression of time-domain diffraction integral

Similar to using the regular operator method in the space domain, in the time domain we also can define the regular

conjugate operator and the regular transform operator. Then the time domain diffraction integration equation (2.12) can be written as the following equations by using the time domain square phase operator Q, Fourier transform operator F, and the scale operator V [11]

$$U_2(\tau_2) = Q[\frac{D}{B}]V[\frac{1}{B}]FQ[\frac{A}{B}]U_1(\tau_1), \quad (B \neq 0) \tag{4.30a}$$

$$U_2(\tau_2) = Q[\frac{C}{A}]V[\frac{1}{A}]u_1(\tau_2), \quad (B = 0) \tag{4.30b}$$

When using the time domain diffraction integration in studying transmission problems of chirp pulses in dispersion medium, it is not required to follow the conventional method for multiple transformation of the time domain and the frequency domain. Furthermore, Eq. (4.30) written in terms of operators can have matrix and operator commutation operations to replace the time-consuming integration computations in the intermediate steps; therefore, the problem is greatly simplified, with the present form, such as [18]:

$$U_1(\tau_1) = E_0 \exp(-2\ln 2\tau_1^2/\Delta t_1^2) \tag{4.31}$$

The time transformation matrix of chirp pulses (Δ_1 is pulse duration and E_0 is constant) is

$$M = \begin{pmatrix} A_1 & B_1 \\ C_1 & D_1 \end{pmatrix} = \begin{pmatrix} 1 & \omega_0 \beta'' z \\ 0 & 1 \end{pmatrix} \tag{4.32}$$

By using transmission in a dispersion medium for explanation, substitute Eq. (4.32) into Eq. (4.30a), and make a computation

operation, thus obtaining

$$U_2(\tau_2)=Q[\frac{1}{B_1}]V[\frac{1}{B_1}]FQ[\frac{1}{B_1}]U_1(\tau_1)=(\frac{1}{A})^{1/2}Q(\frac{C}{A})E_0 \qquad (4.33)$$

In the equation,

$$\begin{pmatrix} A & B \\ C & D \end{pmatrix}=\begin{pmatrix} 1+i\frac{4\ln 2}{\omega_0\Delta t_1^2}B_1 & B_1 \\ i\frac{4\ln 2}{\omega_0\Delta t_1^2} & 1 \end{pmatrix} \qquad (4.34)$$

Thus, we obtain

$$U_2(\tau_2)=\frac{E_0}{(1+\frac{\varphi''^2}{4\Omega^2})^{1/4}}\cdot\exp[-\frac{\tau_2^2}{4\Omega(1+\frac{\varphi''^2}{4\Omega^2})}]\cdot\exp[i\varphi_{out}(\tau_2)] \qquad (4.35)$$

In the equation,

$$\varphi_{out}(\tau_2)=[-\varphi''\tau_2^2/(2\varphi''^2+8\Omega^2)]-\frac{1}{2}\operatorname{arctg}(-\frac{\varphi''}{2\Omega}) \qquad (4.36)$$

$$\Omega=\Delta t_1^2/8\ln 2 \qquad (4.37)$$

$$\varphi''=\beta''z \qquad (4.38)$$

The results obtained are the same as those in [20] and [10]. From Eqs. (4.31) and (4.35), we know that after passing through the pure dispersion medium, the chirp pulse duration Δt is broader, and

$$\frac{\Delta t_2}{\Delta t_1}=(1+\frac{\varphi''^2}{4\Omega^2})^{1/2} \qquad (4.39)$$

With respect to the application examples for B=0 in Eq. (4.30b), these examples can be found in reference [11].

Remark: some contents of the paper were reported in a symposium on the ICF driver technology in Beijing in July 1991. The first draft of the paper was received on September 12, 1991; the final revised draft was received for publication on June 15, 1992.

REFERENCES

[1] 吕百达，胡玉芳等，红外与激光技术，1991, **10**(3): 38 ~ 46.

[2] Born M & Wolf E. Principles of Optics , Pergamon Press, 1975.

[3] Nemoto S. *Appl Opt*. 1990, **29**(13): 1940 ~ 1946.

[4] Rudolf P G, Tollett J J et al. *Appl Opt*. 1990, **29**(7): 998 ~ 1002.

[5] Collins S A. *JOSA*, 1970, **60**(9): 1168 ~ 1177.

[6] Kostenbauder A G. *IEEE J Quant Electron*, 1990, **26**(6): 1148~1157.

[7] 范滇元. 激光, 1980, **7**(8): 26 ~ 35.

[8] 丁桂林，吕百达，量子电子学，1990, **7**(3): 222 ~ 227.

[9] Dijaili S P, Dienes A et al. *IEEE J Quant Electron* , 1990, **26**(6): 1158 ~ 1164.

[10] 张筑虹，范滇元. 光学系统的时间衍射积分及其应用 (光学学报，即将发表).

[11] 丁桂林，吕百达. 时域衍射积分的正则算子表示 (光学学报，即将发表).

[12] 吕百达. 激光光学 . 四川大学出版社，第一版，1986 年，第二版，1992 年.

[13] Luneberg R K, Mathematical Theory of Optics, Uni. California Press, Berkiley, CA. 1964.
[14] Arnaud J A. Hamiltonian Theory of Beam Mode Propagation, in Progress in Optics, Vol. XI. E. Wolf. Ed., North-Holland., Amsterdam, 1973.
[15] Nazarathy M & Shamir J. *JOSA*, 1982,72(3):356~364.
[16] Nazarathy M & Shamir J. *JOSA*, 1982, 72(10):1398~1408.
[17] Kauderer M. *Appl Opt*, 1991, 30(9):1025~1035.
[18] Nazarathy M & Shamir J. *JOSA*, 1981, 71(5):529~541.
[19] Nazarathy M, Hardy A & Shamir J. *JOSA*, 1986, 3(9):1360~1367.
[20] Silvestri S D, Laporta P et al. *IEEE J Quant Electron*, 1984, 20(5):533~538.

DISTRIBUTION LIST

DISTRIBUTION DIRECT TO RECIPIENT

ORGANIZATION	MICROFICHE
B085 DIA/RTS-2FI	1
C509 BALL0C509 BALLISTIC RES LAB	1
C510 R&T LABS/AVEADCOM	1
C513 ARRADCOM	1
C535 AVRADCOM/TSARCOM	1
C539 TRASANA	1
Q592 FSTC	4
Q619 MSIC REDSTONE	1
Q008 NTIC	1
Q043 AFMIC-IS	1
E404 AEDC/DOF	1
E410 AFDTC/IN	1
E429 SD/IND	1
P005 DOE/ISA/DDI	1
1051 AFIT/LDE	1
PO90 NSA/CDB	1

Microfiche Nbr: FTD96C000223
NAIC-ID(RS)T-0510-95